ACS APPLIED MATERIALS & INTERFACES

Research Article

www.acsami.org

Critical Roles of Cationic Surfactants in the Preparation of Colloidal Mesostructured Silica Nanoparticles: Control of Mesostructure, Particle Size, and Dispersion

Hironori Yamada,[†] Chihiro Urata,[†] Sayuri Higashitamori,[†] Yuko Aoyama,[†] Yusuke Yamauchi,[‡,§] and Kazuyuki Kuroda*[,†,¶]

[†]Department of Applied Chemistry, Faculty of Science and Engineering, Waseda University, Ohkubo 3-4-1, Shinjuku-ku, Tokyo 169-8555, Japan

[‡]World Premier International (WPI) Research Center, International Center for Materials Nanoarchitectonics (MANA), National Institute for Materials Science (NIMS), 1-1 Namiki, Tsukuba, Ibaraki 305-0044, Japan

[§]Precursory Research for Embryonic Science and Technology (PRESTO), Japan Science and Technology Agency (JST), 4-1-8 Honcho, Kawaguchi, Saitama 332-0012, Japan

[¶]Kagami Memorial Research Institute for Materials Science and Technology, Waseda University, Nishiwaseda 2-8-26, Shinjuku-ku, Tokyo 169-0051, Japan

Supporting Information

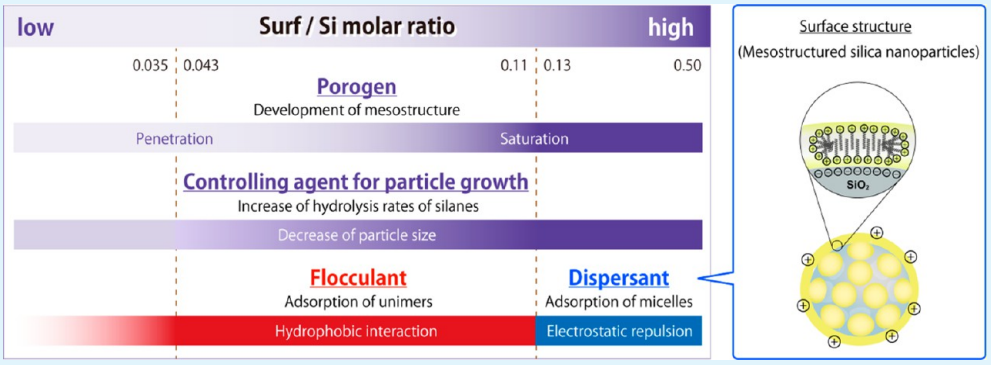

ABSTRACT: Mesoporous silica nanoparticles are promising materials for various applications, such as drug delivery and catalysis, but the functional roles of surfactants in the formation and preparation of mesostructured silica nanoparticles (MSN-as) remain to be seen. It was confirmed that the molar ratio of cationic surfactants to Si of alkoxysilanes (Surf/Si) can affect the degree of mesostructure formation (i.e., whether the mesochannels formed inside the nanoparticles actually pass through the outer surface of the particles), the particle diameter, and the dispersibility of MSN-as. Wormhole-like mesostructures formed with low Surf/Si ratios; however, the mesopores did not pass through the outer surface of the particles completely. At high Surf/Si ratios, the mesostructures extended. The particle diameter was 100 nm or larger at low Surf/Si ratios, and the primary particle diameter decreased as the Surf/Si ratio increased. This was because the surfactants enhanced the dispersity of the alkoxysilanes in water and the hydrolysis rate of the alkoxysilanes became faster, leading to an increased nucleation as compared to the particle growth. Moreover, primary particles aggregated at low Surf/Si ratios because of the hydrophobic interactions among the surfactants that were not involved in the mesostructure formation but were adsorbed onto the nanoparticles. At high Surf/Si ratios, the surfactant micelles were adsorbed on the surface of primary particles (admicelles), resulting in the dispersion of the particles due to electrostatic repulsion. In particular, molar ratios of 0.13 or higher were quite effective for the preparation of highly dispersed MSN-as. Surfactants played important roles in the mesostructure formation, decreasing the particle diameters, and the dispersibility of the particles. All of these factors were considerably affected by the Surf/Si ratio. The results suggested novel opportunities to control various colloidal mesostructured nanoparticles from the aspects of composition, structure, and morphology and will also be useful in the development of novel methods to prepare nanomaterials in various fields.

KEYWORDS: *mesostructured silica nanoparticles, surfactants, particle size, dispersion*

INTRODUCTION

Porous nanoparticles have drawn increasing attention because of the general characteristics of porous materials and the utilization of pores in nanosized particles.[1] In particular,

Received: December 7, 2013
Accepted: January 28, 2014
Published: January 28, 2014

   dx.doi.org/10.1021/am405633r | ACS Appl. Mater. Interfaces 2014, 6, 3491−3500

mesoporous silica nanoparticles (MSN) have been actively prepared as particles with multiple properties including stimuli-responsive, magnetic, and dispersive characteristics, for various applications such as adsorption, separation, catalysis, and drug delivery.[2−17] From the scientific and industrial points of view, it is important to examine the preparation conditions of MSN and their precursors, that is mesostructured silica nanoparticles (MSN-as). MSN-as largely differ from nonporous silica nanoparticles in terms of the utilization of amphiphilic molecules as porogens.

Among amphiphiles, the behavior of molecular surfactants is more clearly explained than that of amphiphilic polymers. Generally, the structure and properties of surfactants vary drastically depending on the critical micelle concentration (CMC). By taking advantage of this property, different kinds of surfactants including cationic, anionic, and nonionic types have been used for the preparation of mesostructured silica.[18−21] Furthermore, surfactants have also been used as dispersants and flocculants of various colloidal particles including colloidal silica[22,23] and as capping agents to control the particle growth of colloidal particles.[22,23] In short, these functions are of great importance from the viewpoint of a controlled formation of highly dispersed MSN-as (same as colloidal mesostructured silica nanoparticles (CMSS), reported previously[24]), which have characteristics of both mesostructured silica and colloidal particles.

Additionally, the pH value of solutions containing silicon sources and surfactants also affects the preparation of MSN-as. Although Palmqvist et al. prepared MSN-as by using the nonionic triblock copolymer Pluronic P123 under acidic conditions,[25] the sol−gel reaction in acidic solutions is not effective for the morphological control of nanoparticles primarily because the reaction leads to the formation of aggregated nanoparticles.[26] Likewise, the use of anionic surfactants is insufficient because they interact with soluble silica species that are cationic under acidic conditions. On the other hand, basic solutions are appropriate for the formation of spherical particles as indicated by the Stöber method.[27] Under these conditions, cationic surfactants can react with anionic soluble silica species effectively. In fact, most reports on the preparation of MSN-as utilize bases and cationic surfactants. We have prepared highly dispersed MSN-as (CMSS) by using alkoxysilanes, a cationic surfactant (cetyltrimethylammonium bromide, C_{16}TMABr), and a base (triethanolamine, TEA).[24,28,29] In particular, we were able to control the particle size of highly dispersed MSN-as in a wide range from *ca.* 20 nm to *ca.* 700 nm by using various kinds of tetraalkoxysilanes and alcohols.[24,28,29] In addition, colloidal mesostructured ethenylene-bridged nanoparticles, which are entirely composed of organosilsesquioxane frameworks, have been prepared using bis(triethoxysilyl)ethenylene.[30] Variation of the hydrolysis rates of the alkoxysilanes can lead to the continuous control of particle diameters. However, it is unclear how cationic surfactants affect mesostructure formation, particle size control, and dispersion of MSN-as, depending on the molar ratio of cationic surfactants to Si, although this is a very critical issue with regard to the scientific understanding and practical applications. Thus, it is quite important to clarify the roles of cationic surfactants in basic solutions for the preparation of MSN-as.

The effect of cationic surfactants on mesostructure, particle diameter, and dispersibility of MSN-as, depending on the molar ratio of cationic surfactants to Si in basic solutions, is reported here. The present study shows that the molar ratio of surfactants to Si is closely related to the roles of the surfactants, as shown in Scheme 1. The surfactants were continuously

Scheme 1. Variation of the Roles of Surfactants and the Structures of Silica Composites, Depending on the Molar Ratios of Surfactants to Si

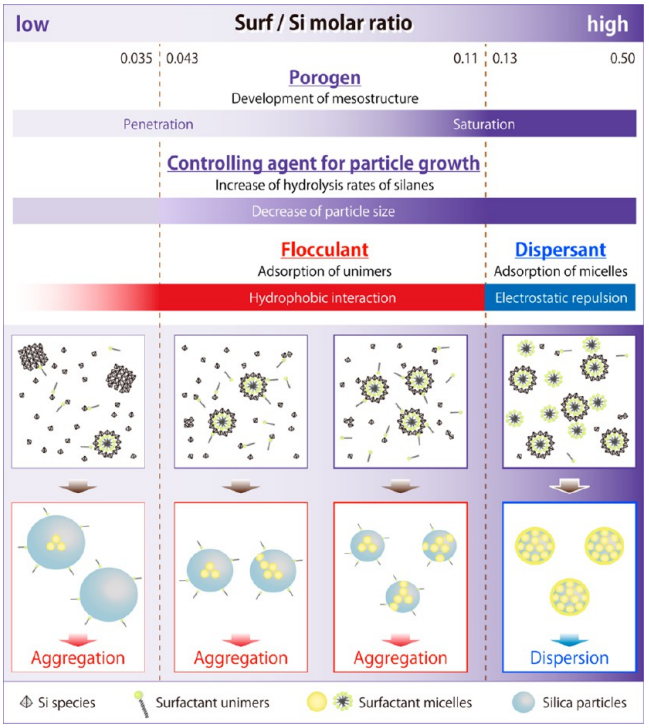

related to the formation of the mesostructure, the decrease of particle diameters, and the dispersion of MSN-as, depending on the molar ratio of surfactants to Si. When higher molar ratios were utilized, particles were dispersed because of the electrostatic repulsion from the adsorption of surfactant micelles on the surfaces of the primary particles. In particular, the condition of high molar ratios of surfactants to Si was quite effective for the formation of highly dispersed MSN-as.

Likewise, MSN-as were prepared by using cationic surfactants with pyridinium rings that could be detected by UV−vis spectroscopy. The amount of the surfactants interacting with silica and the amount of the free surfactants in solution were quantified. From this result, it was demonstrated that the structural state of the surfactants, adsorbed on the surface of the particles, was relevant to the dispersibility of the MSN-as. It was also shown that the structural model for the surfactant adsorption on the surface of particles in an admicelle state[31,32] was applied to the MSN-as. This model was also supported by the difference observed in the dispersion/aggregation behavior on varying the way of ethanol addition.

Consequently, the roles of surfactants on the design of MSN-as were shown in an integrated form, through a comprehensive examination of the formation of MSN-as by focusing on the ratio of the surfactants to the inorganic species. Although herein we focus mainly on the MSN-as, we believe that the information reported here can contribute to the selective development of preparation methods of nanomaterials with

Scheme 2. Brief Scheme for the Preparation of Mesostructured Silica Nanoparticles (MSN-R-as) and Mesoporous Silica Nanoparticles (MSN-R-cal) with Different Molar Ratios *R* of C_{16}TMABr to Si

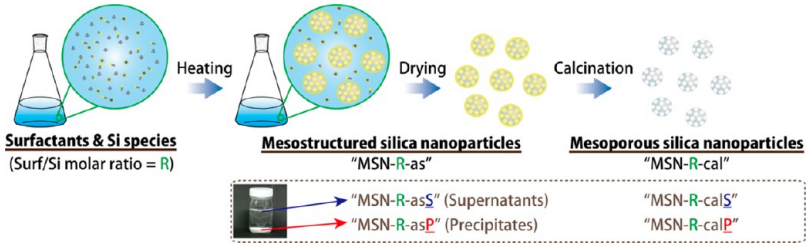

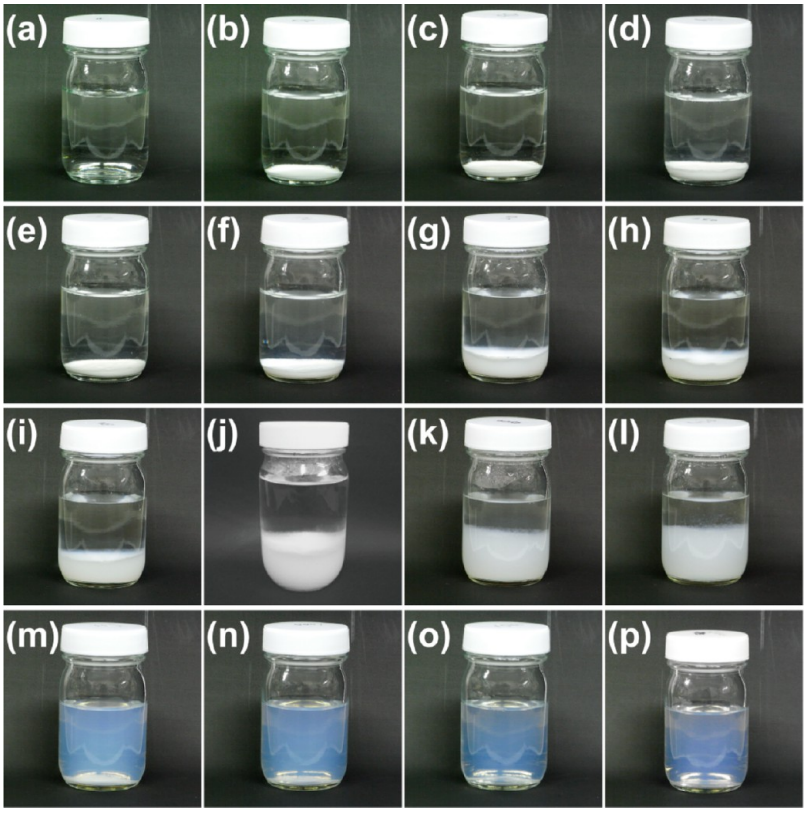

Figure 1. Variation in the appearances of solutions (a) nMSN and (b–p) MSN-R-as with different molar ratios (*R*; C_{16}TMABr to Si). The values are (b) 0.013, (c) 0.020, (d) 0.028, (e) 0.035, (f) 0.043, (g) 0.050, (h) 0.063, (i) 0.075, (j) 0.086, (k) 0.10, (l) 0.11, (m) 0.13, (n) 0.25, (o) 0.38, and (p) 0.50, respectively.

regard to the control of mesostructure, particle size, and dispersion.

EXPERIMENTAL SECTION

Materials. Octyltrimethylammonium bromide (C_8TMABr), decyltrimethylammonium bromide (C_{10}TMABr), dodecyltrimethylammonium bromide (C_{12}TMABr), tetradecyltrimethylammonium bromide (C_{14}TMABr), hexadecyltrimethylammonium bromide (C_{16}TMABr), octadecyltrimethylammonium bromide (C_{18}TMABr), hexadecylpyridinium chloride (C_{16}PyCl), triethanolamine (TEA), and acetic acid were purchased from Wako Pure Chem. Ind., Ltd. Tetraethoxysilane (TEOS: $Si(OC_2H_5)_4$) was purchased from Tokyo Kasei Co., Ltd. All chemicals were used as received without further purification.

Characterization. UV–vis spectra of the colloidal nanoparticles were obtained using a Shimadzu UV-2500PC spectrophotometer. TEM images were obtained on a JEOL JEM-2010 microscope operating at 200 kV. The samples for the TEM measurements were dropped and dried on a carbon-coated microgrid (Okenshoji Co.). Zeta potential measurements were conducted with an Otsuka Electronics ELSZ-1 at 20 °C. The state of the samples for the zeta potential measurements was (colloidal) solution. (Actually, as for our solid samples, the potential measurements were neither stabilized nor reproducible. So, reliable data were not obtained.) The X-ray diffraction (XRD) patterns of dried powder samples were obtained on a RIGAKU Nano-Viewer. Nitrogen gas adsorption–desorption measurements were performed using an Autosorb-2 instrument (Quantachrome Instruments) at −196 °C. Samples were preheated at 120 °C for 24 h under 1×10^{-2} Torr. Brunauer–Emmett–Teller (BET) surface areas were calculated from the adsorption data in a relative pressure range from 0.05 to 0.20. The concentrations of Si species in supernatant solutions were determined by an inductively coupled plasma (ICP) spectrometer with a Vista-MPX instrument (Varian Technology Japan Ltd.) after filtering with a Millipore filter (0.45 μm).

Preparation of MSN-as. A brief scheme for the preparation of MSN is shown in Scheme 2. First, TEOS was hydrolyzed and condensed under basic conditions as reported previously.[28] TEA (0.420 g), C_{16}TMABr (0.143–5.5 mmol), and 240 mL of water were mixed, and the solution was stirred at 80 °C for 2 h. Then, 11 mmol of TEOS was added to the solution with vigorous stirring at 80 °C for 8 h. The evaporation was prevented by simply covering with an Al foil.

The molar ratio of the precursor solution was 1 TEOS:0.013−0.50 C_{16}TMABr:0.25 TEA:1200 H_2O. These nonpercolated solutions were named as MSN-R-as, where "*R*" is the molar ratio of C_{16}TMABr to Si. After the reaction was complete, all solutions were filtered using No. 5 filter paper to remove impurities like dusts possibly involved during the processes. When the value of *R* was less than 0.13, precipitates were recovered. When the *R* values were 0.013−0.035 and 0.13−0.50, supernatants were collected. These filtered samples were denoted as MSN-R-asP or MSN-R-asS, respectively, where "P" indicates precipitates and "S" indicates supernatants. Then, these samples were dried at 120 °C for 12 h, followed by calcination at 550 °C for 6 h. The calcined samples were named as MSN-R-calP, or MSN-R-calS. In addition, colloidal nanoparticles were prepared from TEA, water, and TEOS without surfactants; that is, the value of *R* was zero. Herein, this is denoted as "nMSN" which means nonmesoporous silica nanoparticles. (Note: Even if the samples did not have a complete mesostructure, the expression "MSN" is used throughout. For example, it is used when *R* is less than 0.13.)

Investigation of Free Surfactants in the Colloidal Solution. MSN-as were prepared as described above by using C_{16}PyCl, which has a pyridinium ring detectable in the UV region (259.2 nm), as a surfactant instead of C_{16}TMABr, in molar ratios of 0.050, 0.086, 0.13, 0.19, 0.26, 0.32, 0.39, 0.45, and 0.50 (C_{16}PyCl to Si). Surfactants used in the preparation of MSN-as were divided into two groups: "composite surfactants" and "free surfactants". The former refers to those that were adsorbed on the surface of the particles, or acted as porogens inside the particles, and the latter indicates those that were in solution and not adsorbed. In order to quantify the ratio of these two groups of surfactants, the separation process, shown in Scheme S1, Supporting Information, was conducted. Through centrifugation using centrifuge tubes with a membrane filter (MWCO = 100 k), the two types of surfactants can be separated: composite surfactants were present in the upper portion, and free surfactants were present in the lower portion. Although some free surfactants remained in the upper part, the concentration of the free surfactants in the lower portion could be regarded as the same as that of the free surfactants in the upper portion. Thus, the amounts (and the ratio) of those surfactants could be quantitatively determined by measuring the UV absorbance of the surfactants in the lower portion. On the basis of these values, the functions of the surfactants are discussed in the following section, in accordance with the molar ratio of surfactants to Si.

Effect of the Addition of Ethanol on Colloidal Dispersity of MSN-as. The colloidal dispersity of MSN-as was investigated in two ways: ethanol (5.0 mL) was added to MSN-0.50-as (5.0 mL) (i) without acetic acid and (ii) after the addition of acetic acid and the adjustment of pH value. Likewise, the dispersity of colloidal mesostructured nanoparticles with ethenylene-bridged silsesquioxane frameworks (MSqN-0.50-as), which were prepared according to the previous report,[30] were also investigated. The colloidal dispersity was estimated by monitoring whether aggregates were formed when the state of the solution was varied.

Preparation of MSN-as with Several Alkyltrimethylammonium Bromides. MSN-as were prepared using several alkyltrimethylammonium bromides (C_8TMABr, C_{10}TMABr, C_{12}TMABr, or C_{14}TMABr) except C_{16}TMABr when the molar ratio of surfactants/Si was 0.50. These samples were denoted as CY-0.50, where "CY" indicates the number of carbons in the surfactant, and "0.50" indicates the molar ratio of the surfactants to Si. For example, in the case of C_{10}TMABr, the sample was denoted as "C10−0.50".

RESULTS AND DISCUSSION

1. Effect of the Molar Ratio of Surfactants to Si on the Formation of MSN-as. Figure 1 shows the appearances of the solutions depending on the molar ratio *R* of C_{16}TMABr to Si. When *R* was 0.013−0.035, dispersed and precipitated particles coexisted in the as-prepared solutions. When *R* was 0.043−0.11, only precipitated particles were observed, and when *R* was 0.13−0.50, precipitates were not observed; that is, particles were highly dispersed. This phenomenon corresponded nicely to the Si concentration in the supernatants as shown in Figure 2. Being different from the concentration of the initially loaded

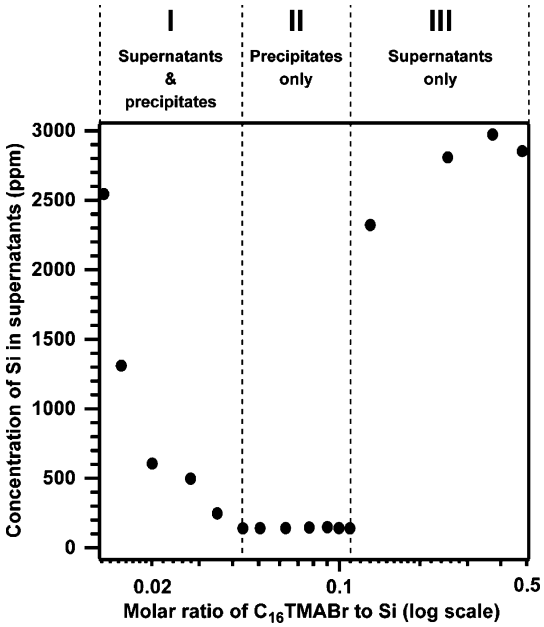

Figure 2. Concentration of Si in supernatants with different molar ratios of C_{16}TMABr to Si. Except for the case without surfactants (that is, when the molar ratio of C_{16}TMABr to Si is zero), the concentration is divided into three regions: region I, from 0.013 to 0.035; region II, from 0.043 to 0.11; and region III, from 0.13 to 0.50, where the number indicates the molar ratios of C_{16}TMABr to Si.

Si, which remained almost constant (2750 ppm), the Si concentration in the supernatants varied widely from 200 to 1300 ppm in region I. This wide range indicates that Si species were present in both the supernatants and precipitates. In this region, the Si concentration in the supernatants was lower, as the value of *R* was higher. In region II, the concentrations were almost the same at around 100 ppm. This means that most of the Si species were present in the precipitates. In region III, the value was *ca.* 2500 ppm, indicating that most of the Si species were present in the supernatants in their colloidal states, and therefore, the particles were highly dispersed. The effect of *R* on the formation of colloidal mesostructured silica nanoparticles is discussed in the following sections by dividing the values of *R* into three groups, low (*R* = 0.013−0.035), middle (*R* = 0.043−0.11), and high (*R* = 0.13−0.50) values. When *R* was zero, nonporous silica nanoparticles were formed. (Note: In order to show clearly the mesostructure of silica nanoparticles, enlarged TEM images are shown in Figure S1, Supporting Information.)

1.1. C_{16}TMABr/Si = 0.013−0.035. As shown in Figure 1b−e, precipitates were observed when a small amount of surfactant was present in the solutions. In this case, the hydrophobic alkyl chains of surfactants adsorbed in monolayers on the surfaces of particles and were assembled in aqueous systems due to the hydrophobic interactions. Surfactants acted as flocculants, and the particles aggregated. This will be discussed in this section later. TEM images of precipitates (Figure 3b-2−e-2) show that the particle diameter decreased from *ca.* 500 nm to *ca.* 20 nm as the molar ratio of surfactants increased. The images also show the presence of mesostructures. The XRD patterns (Figure 4) of the calcined precipitates show broad peaks around $2\theta = 2°$, and this also suggests the formation of mesostructures. BET

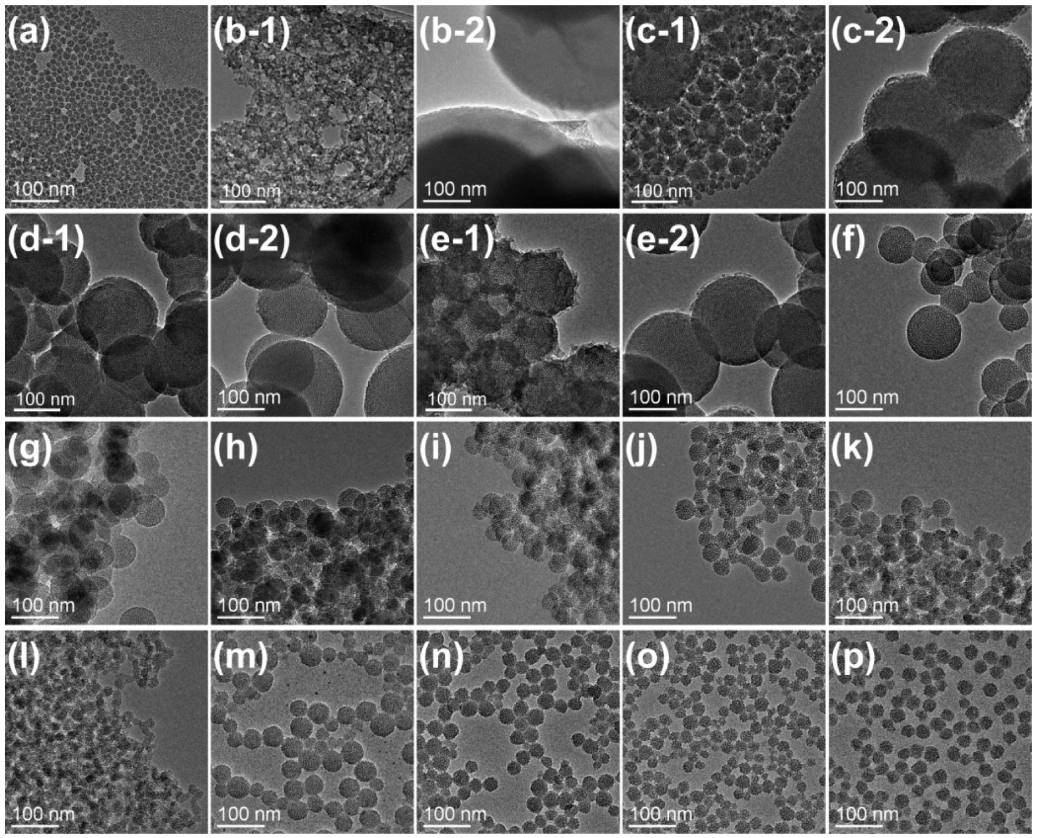

Figure 3. Variation in the TEM images of (a) nMSN, (b−p) supernatants and precipitates of MSN-R-as with different molar ratios, *R*, of C_{16}TMABr to Si: (a) nMSN, (b-1) MSN-0.013-asS, (b-2) MSN-0.013-asP, (c-1) MSN-0.020-asS, (c-2) MSN-0.020-asP, (d-1) MSN-0.028-asS, (d-2) MSN-0.028-asP, (e-1) MSN-0.035-asS, (e-2) MSN-0.035-asP, (f) MSN-0.043-asP, (g) MSN-0.050-asP, (h) MSN-0.063-asP, (i) MSN-0.075-asP, (j) MSN-0.086-asP, (k) MSN-0.10-asP, (l) MSN-0.11-asP, (m) MSN-0.13-asS, (n) MSN-0.25-asS, (o) MSN-0.38-asS, and (p) MSN-0.50-asS, where S and P denote supernatants and precipitates, respectively.

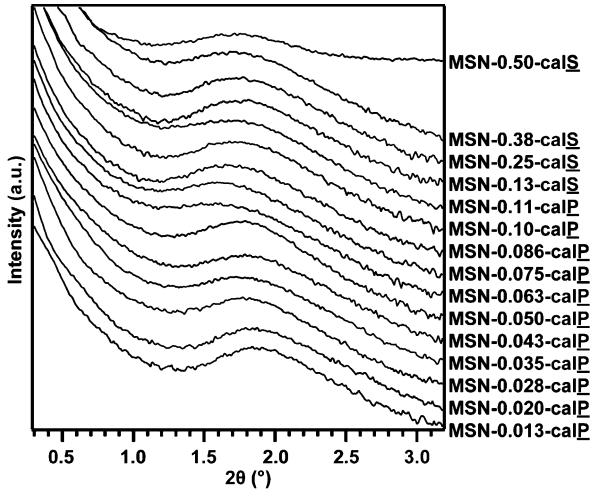

Figure 4. Variation in the XRD patterns of calcined samples with different molar ratios, *R*, of C_{16}TMABr to Si. In the calcined sample names given on the right, S and P denote supernatants and precipitates, respectively, and the number indicates the value of *R*.

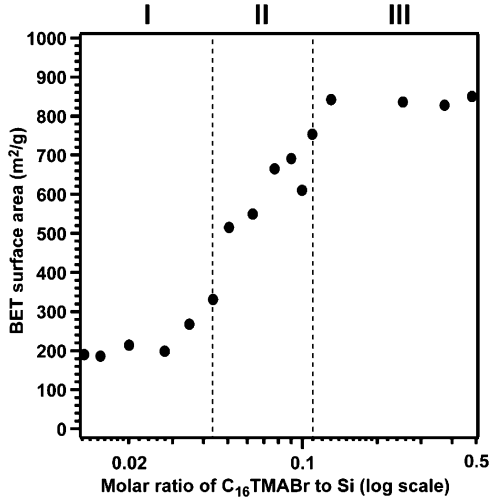

Figure 5. Variation in the BET surface areas of calcined samples with different molar ratios of C_{16}TMABr to Si. Region I ranges from 0.013 to 0.035, region II from 0.043 to 0.11, and region III from 0.13 to 0.50, where the number indicates the molar ratios of C_{16}TMABr to Si.

surface areas (Figure 5) calculated from the N_2 adsorption isotherms were almost the same (ca. 200−300 m^2/g), and considerably high surface areas were not revealed despite mesostructure formation. On the basis of these results, the formation of mesostructured silica nanoparticles, when low molar ratio of cationic surfactants to Si of alkoxysilanes (Surf/Si) were utilized, is explained as follows: First, some surfactants formed composites with hydrolyzed alkoxysilanes because of electrostatic interactions, which formed the nuclei of the mesostructured materials. As the *R* value increased, the alkoxysilanes were more easily dispersed in solution as oils[26] and the hydrolysis of alkoxysilanes proceeded more readily.

dx.doi.org/10.1021/am405633r | ACS Appl. Mater. Interfaces 2014, 6, 3491−3500

Thus, the nucleation of mesostructured materials dominated the growth, and the particle diameter decreased.[28,29] This phenomena was promoted by the increase of the R value. Surfactants acted as porogens of mesostructured silica nanoparticles until the surfactants were consumed, and this was related to the amount of Si. Even when the amount of surfactants did not meet the required amount to act as a porogen, the amount of alkoxysilanes was sufficient for the formation of nonporous silica on the surface of the existing mesostructured materials. This meant that the mesostructures formed only in the initial stage and did not always extend to the outer surface of the particles; thus, high surface areas due to mesopore formation were not observed. In fact, the TEM images (typically Figure S1a, Supporting Information) show the presence of some rough layers which do not contain mesostructural contrasts. These results are consistent with those reported previously on the plugged hexagonal template silica and plugged SBA-15.[33−36] In addition, surfactants which were not involved in the formation of templates could interact with Si species or silica nanoparticles. Thus, unimers of such surfactants were adsorbed as a monolayer on the surface of the particles, and hydrophobic alkyl chains derived from surfactants were exposed in solution, leading to the aggregation of primary particles because of the hydrophobic interactions. The nonporous silica layers were also likely formed on these aggregates.

On the other hand, the XRD patterns (data not shown) of the calcined samples derived from the supernatants, where R = 0.013−0.035, indicated that the mesostructures were not observed clearly. The TEM images of the samples in Figure 3b-1−e-1 show the mesostructures of particles, which is somewhat inconsistent with the XRD results. However, the main products were present in the precipitates in region I, corresponding to the Si concentrations in Figure 2. In other words, the structures observed in the TEM images of the samples derived from the supernatants did not reflect the state of the main products, so the discussion on these structures is excluded.

The surfactants worked as porogens depending on the amount of Si, and mesostructured silica nanoparticles were formed until the surfactants were consumed. When the amount of the surfactants was not sufficient for its action as a porogen, colloidal nonporous silica nanoparticles or nonporous silica layers were formed on the mesostructured silica nanoparticles. In addition, the surfactants, which did not act as porogens and did not form micelles, acted as flocculants of nonporous and mesoporous silica nanoparticles. As mentioned above, silica layers were also formed on the aggregates.

1.2. C_{16}TMABr/Si = 0.043−0.11. The results of Figures 1f−l and 2 indicate that almost the entire Si formed precipitates in the middle region II. The TEM images of the precipitates in Figure 3f−l show that the particle diameter decreased relatively, as the ratio of the surfactants increased. As mentioned in Section 1.1, this can be explained by relating the surfactant ratios to the hydrolysis rates of alkoxysilanes. The XRD patterns (Figure 4) of the calcined precipitates show broad peaks around 2θ = 2°, and this suggests the formation of mesostructures. BET surface areas (Figure 5) calculated from the N_2 adsorption isotherms gradually increased as the molar ratio of the surfactants increased. This result shows that most surfactants played a role in the formation of mesostructures as porogens; thus, the mesostructures and pores passed through the outer surface of the particles. Additionally, those particles had wormhole-like mesostructures, regardless of the ratio of the surfactants. This means that the assembly of the silica species and surfactants did not depend on the ratio of the surfactants. Moreover, the surfactants, which were not related to the formation of mesostructures, contributed to the aggregation of particles due to hydrophobic interactions, as described in Section 1.1. The surface charge of the silica nanoparticles was negative because of the Si species, but the surfactants located/adsorbed on the outer surfaces acted as flocculants. From these results, it is confirmed that, in region II, the surfactants acted as porogens, as controlling agents for particle growth, and as particle flocculants.

1.3. C_{16}TMABr/Si = 0.13−0.50. Finally, in region III, precipitates were not observed and each colloid had high transparency and dispersibility, as shown in Figure 1m−p. This was supported by the high Si concentration in the supernatants and in the mother solution (Figure 2). The TEM images shown in Figure 3m−p reveal the formation of particles with mean diameters *ca.* 30 nm, though the relationship between the ratio of the surfactants and particle diameters was not confirmed, as indicated in the regions I and II. The XRD patterns (Figure 4) of the calcined samples show broad peaks around 2θ = 2° because of the formation of mesostructures. The BET surface areas (Figure 5) were high (800 m^2/g), while all surfactants were not used for the formation of mesostructures. In other words, even after the mesostructures were fully formed, a certain amount of the surfactants was still present in the solution. In fact, when these colloids were cooled, the crystals derived from the surfactants precipitated (as shown in Figure S2, Supporting Information) and the crystals disappeared when the colloids were heated. This process could be repeated without the formation of aggregated nanoparticles. This shows that excess amounts of surfactants, excluding those which were related to the formation of the mesostructures, were contained in the colloid. The representative zeta potentials of these colloids (Table 1) were positive, meaning that the surface of particles is charged positively (including mesostructured nanoparticles, shown later in Section 2.1). Each zeta potential was positive; however, all data are not shown here. Because of the electrostatic repulsion of cationic surfaces, high dispersibility of the mesostructured silica nanoparticles was retained.

Table 1. Zeta Potential Values of Solutions with Different Molar Ratios of C_{16}TMABr to Si: MSN-0.13-as<u>S</u>, MSN-0.25-as<u>S</u>, MSN-0.38-as<u>S</u>, and MSN-0.50-as<u>S</u>

sample	ζ-potential (mV)
MSN-0.13-as<u>S</u>	+49
MSN-0.25-as<u>S</u>	+53
MSN-0.38-as<u>S</u>	+44
MSN-0.50-as<u>S</u>	+53

2. Surface States of MSN-as. *2.1. Effect of the Presence of "Free Surfactants" on the Dispersity of MSN-as.* By using surfactants containing pyridinium rings, C_{16}PyCl rather than C_{16}TMABr, MSN-as were prepared. In this section, the concentrations of two kinds of surfactants were investigated by separating nanoparticles from solution (Scheme S1, Supporting Information); some surfactants were related to the formation of the mesostructures (composite surfactants), and the others were not related (free surfactants). The appearances of MSN-as prepared by using different ratios of the surfactants to Si were similar to those of C_{16}TMABr (Figure

S3, Supporting Information). Precipitates formed at ratios lower than 0.13, and colloids were obtained at ratios of 0.13 or higher. However, at the ratio of 0.13, the colloidal solution prepared from C_{16}PyCl was a little bit cloudier than that prepared from C_{16}TMABr, indicating the effect of the kind of surfactants on the dispersity of MSN-as at the very critical molar ratio.

In addition, the particle diameters decreased prominently in the region of 0.050 to 0.13 (Figure S4, Supporting Information). These solutions were measured by UV−vis spectroscopy after separating the nanoparticles from the solutions. The concentrations of the composite and free surfactants are shown in Figure 6. It was confirmed that, as the

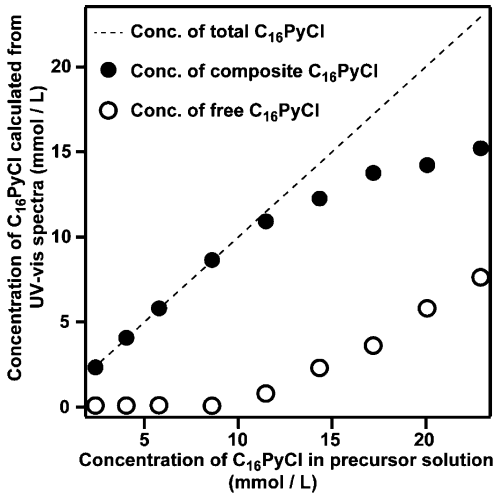

Figure 6. Relationship between the concentration of C_{16}PyCl calculated from UV−vis spectra (mmol/L) and that of the precursor solution (mmol/L).

ratio increased, the amount of the composite surfactants approached a constant value and that the amount of the free surfactants increased continually. The zeta potentials of the solutions were positive, and the surface of MSN-as had a positive charge at pH 8.2. The results of Figures 6, S3, and S4, Supporting Information, indicate that, when the particles were aggregated (when the ratio was lower than 0.13), the amount of free surfactants was quite small, and when the particles were dispersed (when the ratio was 0.13 or higher), free surfactants were present in these colloids. The micelles of the surfactants, which were not related to the formation of mesostructures, were adsorbed on the surface of the particles; thus, the particles with cationic surfaces were dispersed because of the electrostatic repulsion. This aspect is discussed in Section 2.3. The ratio of the surfactants to Si (0.13) is critical for the stable dispersion of MSN-as. Consequently, although secondary particles were formed when ratios near 0.13 were utilized, the micelles of the surfactants acted as dispersants when the ratio of the surfactants was higher than a constant value.

2.2. Effect of Critical Micelle Concentration (CMC) of Several Alkyltrimethylammonium Surfactants on the Formation of Highly Dispersed MSN-as. Next, the effect of the critical micelle concentration (CMC) on the dispersion state of the particles was investigated. As the length of the alkyl chain increased, the CMC of the surfactants decreased and it was easier to form micelles. Concentrations and CMCs of surfactants with different alkyl chain lengths used here are shown in Table 2.[31,37] White precipitates were observed when the concentrations of the surfactants were lower than their

Table 2. Zeta Potential Values and Other Properties of Solutions Prepared from Surfactants with Different Alkyl Chain Lengths: C10-0.50, C12-0.50, C14-0.50, C16-0.50, and C18-0.50

C*n*	CMC (mmol/L)[a]	conc. (mmol/L)	ζ-potential (mV)	dispersity
C*10*	66.6	22.8	(N.D.)	×
C*12*	14.6	22.8	+53	○
C*14*	3.72	22.8	+42	○
C*16*	0.90	22.8	+53	○
C*18*	0.31	22.8	+43	○

[a]Refs 31 and 37.

CMCs (Figure 7). However, in the case of C_{18}TMABr, the colloidal solution was a little cloudier than that prepared from C_{16}TMABr. Even though the real concentrations of the used surfactants are the same, the gap between the concentrations and CMC should be largest for C_{18}TMABr. Consequently, the fraction of micelles should be more than the cases of other surfactants, resulting in the cloudier phenomenon, though the details remain to be clarified. As seen in the TEM images (Figure S5, Supporting Information), the particle diameter decreased as the CMC of the surfactant decreased. This means that the use of the surfactants with low CMCs is effective for the formation of highly dispersed MSN-as. Even in the case of C_{10}TMABr, when the concentration of the surfactants was higher than the CMC, the dispersed nanoparticles were obtained (data not shown).

2.3. Proposed Structure of Surfactants Adsorbed on MSN-as. The admicelles of surfactants should be adsorbed on the surface of MSN-as, as shown in Scheme 3. This admicelle structure was proposed as a model of micelles on the surface of silica; this was not a bilayer structure but represented a slightly deformed micelle on the basis of spectroscopic results.[31,32] According to this model, the preparation conditions for obtaining highly dispersed MSN-as are discussed with regard to dispersion/aggregation behavior induced by the addition of ethanol to MSN-as with or without acetic acid.

It is important to understand how colloidal nanoparticles are dispersed in aqueous media for the utilization of nanoparticles. As-prepared samples in this study had high transparency, and the nanoparticles were dispersed. It was reported that the addition of alcohol to such colloids in aqueous media leads to the aggregation of nanoparticles.[38,39] Likewise, we confirmed that the addition of ethanol to MSN-0.50-as led to the production of white precipitates (Figure 8). This was due to the addition of ethanol, which led to the partial breakage of admicelle-type C_{16}TMA protective layers, but the single layers of C_{16}TMA on the surfaces of the nanoparticles were retained; this led to the hydrophobic interaction of the alkyl chains of the surfactants (Scheme 3). However, after the pH of MSN-0.50-as was adjusted to the isoelectric point (pI) of silica or lower, by adding a moderate amount of acetic acid, precipitates were not produced despite the addition of ethanol. At pH values close to the isoelectric point of silica or lower, the electrostatic interaction between the surface of silica and the C_{16}TMA ion was negligible. Thus, the C_{16}TMA layers were desorbed from the surfaces of the nanoparticles, and the hydrophilic surfaces were exposed, followed by the suppression of the aggregation of the nanoparticles.

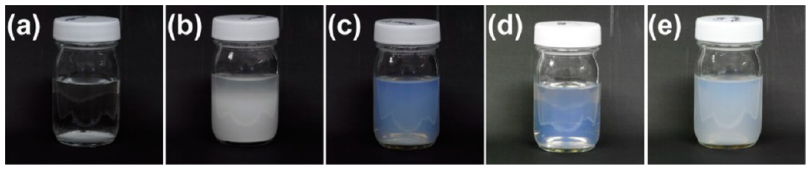

Figure 7. Variation in the appearances of solutions prepared from surfactants with different alkyl chain lengths: (a) C10−0.50, (b) C12−0.50, (c) C14−0.50, (d) C16−0.50, and (e) C18−0.50.

Scheme 3. Proposed Model of Dispersion/Aggregation Behavior Induced by the Addition of Ethanol and/or Acetic Acid to MSN-as

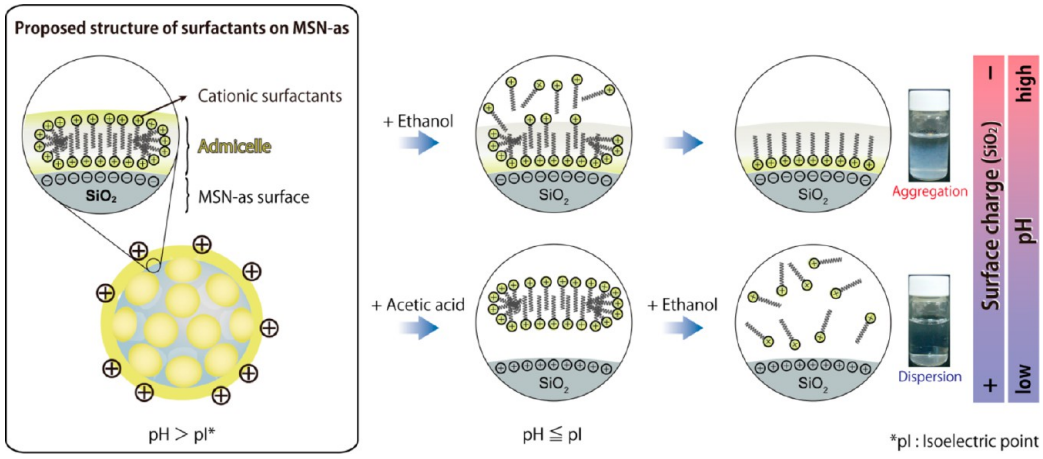

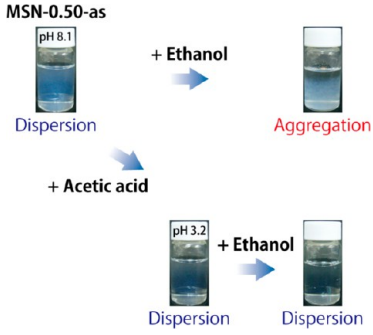

Figure 8. Appearances of dispersion/aggregation behavior induced by the addition of acetic acid and/or ethanol to MSN-0.50-as.

The pH of MSN-0.50-as was adjusted by adding acetic acid. Subsequently, ethanol was added, and the resulting appearance of MSN-0.50-as is shown in Figure S6a, Supporting Information. There was a mixture of dispersed and aggregated particles of MSN-0.50-as between pH 3.6 and 4.0. This pH value is denoted as the "critical aggregation pH" here. Similar to a previous report on colloidal mesostructured organosilsesquioxane nanoparticles,[30] the dispersion−aggregation state was examined. In this case, the critical aggregation pH was 7.4−8.0 as shown in Figure S6b, Supporting Information. This value was higher than that of MSN-as. This was because the acidity of the silanol groups in the ethenylene-bridged silsesquioxane frameworks was lower than that of the siloxane frameworks. This indicates the importance of adjusting the surface charge in accord with the composition of the siloxane frameworks when surfactants are extracted by ethanol without the aggregation of particles, as suggested previously with regard to the retention of the colloidal state of mesoporous silica and organosiloxane nanoparticles.[24,28−30]

3. Other Notes on the Critical Roles of Cationic Surfactants in the Preparation of MSN-as. Even when colloidal particles aggregate, their colloidal properties can be utilized sufficiently if they are redispersed. It has been reported that MSN has high redispersity in water by modifying the surface of MSN.[40] On the other hand, in the present study, after the removal of surfactants of precipitated MSN-as in regions I and II by acid treatment, they were not redispersed even when the pH values were varied to any values. Furthermore, when surfactants were added to as-made MSN solutions, MSN-as were not redispersed. This should be because some silanol groups of primary MSN-as were condensed during the reaction at 80 °C. Moreover, when the aggregation of MSN-as occurred under the thermal condition at 80 °C, the condensation between silanol groups on particles would occur more preferentially than in the case of non-aggregated MSN-as under the same condition.

The condensation of silanol groups between particles should occur on the surfaces of particles which are not fully covered with surfactants. The structural model of surfactants adsorbed on MSN-as is shown in Scheme 3, but surfactants should not fully cover the surfaces of MSN-as. If the aggregation of MSN-as had occurred only due to hydrophobic interactions of alkyl chains of surfactants, MSN-as could have been redispersed. TEA, which was used as a base in this study, plays a role in the restriction of the growth and aggregation of silica particles by forming silatrane structures, as is known.[2,41,42] TEA should have the same effect also in this study and may be adsorbed partly on the surfaces of MSN-as. However, as long as the present study is concerned, the effect of TEA on the particle size should be less than that of surfactants because the concentration of TEA is constant.

In addition to redispersity, it is important to increase the yield of colloidal particles for practical applications. In this

study, the yield of each batch, combining both precipitates and supernatants, was over 90%. Even though the yield was quite high, the weight ratio of MSN-as was around 0.35 wt % in the present study. Higher concentrations of both silica sources and surfactants would increase the weight ratio, but such variations should inevitably cause aggregation though the effect on the decrease in the size of mesoporous silica particles was reported.[43] Although it is still difficult to prepare highly dispersed and small MSN-as under high concentrations of Si sources and surfactants at the present stage, the difficulty may be overcome by simple concentration of colloidal solutions after preparing initial ones.[30]

As a consequence, the surface structure of MSN-as can be most reasonably explained by adopting the model of admicelles to this system. The results on the several functions of the surfactants were systematically organized for the formation of highly dispersed MSN-as at appropriate Si concentrations. This information is quite useful not only for the precise control of colloidal mesostructured and mesoporous silica nanoparticles in terms of particle diameter, structure, and dispersibility but also for the preparation of colloidal mesoporous nanoparticles with other compositions. Thus, mesostructure and dispersibility of nanoparticles can be controlled by varying the molar ratio of surfactants to the structural elements.

CONCLUSIONS

Surfactants have various functional roles depending on their molar ratio to Si in the formation and preparation of mesostructured silica nanoparticles. The major four roles of surfactants found here are as porogens, controlling agents of particle size, flocculants, and dispersants. (i) At low Surf/Si ratios, the surfactants mainly acted as porogens. The mesopores did not pass through the surface of the particles because of the shortage of the surfactant. Another role was as flocculants but the degree was not complete because of the shortage of the surfactant. (ii) In the medium Surf/Si ratio range, three functions of surfactants were noted including its function as porogens (mesopores were further developed), particle size controllers, and flocculants. (iii) In the high ratio range, the surfactants acted as porogens and dispersants. Though each role of the surfactants was individually identified in previous studies, multiple roles are clarified herein systematically for the first time. These findings may promote the logical and strategic preparation of colloidal mesoporous silica nanoparticles, with a precise control to obtain uniform particle sizes. In addition, the information should be helpful for the preparation of nanomaterials made from not only silica but also other compositions; this can lead to the development of various materials having both porous and nanoscale properties through preparation using amphiphiles.

ASSOCIATED CONTENT

Supporting Information

Figures of TEM images and variations in the appearances of the precipitates/solutions of MSN-as; scheme of the separation process of composite and free C_{16}PyCl by centrifuation with a membrane filter. This material is available free of charge via the Internet at http://pubs.acs.org.

AUTHOR INFORMATION

Corresponding Author

*Fax: +81-3-5286-3199. Tel: +81-3-5286-3199. E-mail: kuroda@waseda.jp.

Notes

The authors declare no competing financial interest.

ACKNOWLEDGMENTS

The authors thank Mr. M. Fuziwara (Waseda University) for his kind assistance with the acquisition of the TEM images. This work was supported in part by the Elements Science and Technology Project, "Functional Designs of Silicon−Oxygen-Based Compounds by Precise Synthetic Strategies" and the Grants for Excellent Graduate Schools (Practical Chemical Wisdom), MEXT, Japan.

REFERENCES

(1) Valtchev, V.; Tosheva, L. Porous nanosized particles: Preparation, properties, and applications. *Chem. Rev.* **2013**, *113*, 6734−6760.
(2) Möller, K.; Kobler, J.; Bein, T. Colloidal suspensions of nanometer-sized mesoporous silica. *Adv. Funct. Mater.* **2007**, *17*, 605−612.
(3) Lee, J. E.; Lee, N.; Kim, T.; Kim, J.; Hyeon, T. Multifunctional mesoporous silica nanocomposite nanoparticles for theranostic applications. *Acc. Chem. Res.* **2011**, *44*, 893−902.
(4) Ambrogio, M. W.; Thomas, C. R.; Zhao, Y.-L.; Zink, J. I.; Stoddart, J. F. Mechanized silica nanoparticles: A new frontier in theranostic nanomedicine. *Acc. Chem. Res.* **2011**, *44*, 903−913.
(5) Bitar, A.; Ahmad, N. M.; Fessi, H.; Elaissari, A. Silica-based nanoparticles for biomedical applications. *Drug Discovery Today* **2012**, *17*, 1147−1154.
(6) Li, Z.; Barnes, J. C.; Bosoy, A.; Stoddart, J. F.; Zink, J. I. Mesoporous silica nanoparticles in biomedical applications. *Chem. Soc. Rev.* **2012**, *41*, 2590−2605.
(7) Vivero-Escoto, J. L.; Huxford-Phillips, R. C.; Lin, W. Silica-based nanoprobes for biomedical imaging and theranostic applications. *Chem. Soc. Rev.* **2012**, *41*, 2673−2685.
(8) Yang, P.; Gai, S.; Lin, J. Functionalized mesoporous silica materials for controlled drug delivery. *Chem. Soc. Rev.* **2012**, *41*, 3679−3698.
(9) Yokoi, T.; Kubota, Y.; Tatsumi, T. Amino-functionalized mesoporous silica as base catalyst and adsorbent. *Appl. Catal., A* **2012**, *421*−*422*, 14−37.
(10) Wu, K. C.-W.; Yamauchi, Y. Controlling physical features of mesoporous silica nanoparticles (MSNs) for emerging applications. *J. Mater. Chem.* **2012**, *22*, 1251−1256.
(11) Chen, Y.; Chen, H.; Shi, J. In vivo bio-safety evaluations and diagnostic/therapeutic applications of chemically designed mesoporous silica nanoparticles. *Adv. Mater.* **2013**, *25*, 3144−3176.
(12) Mamaeva, V.; Sahlgren, C.; Lindén, M. Mesoporous silica nanoparticles in medicine-recent advances. *Adv. Drug Delivery Rev.* **2013**, *65*, 689−702.
(13) Tarn, D.; Ashley, C. E.; Xue, M.; Carnes, E. C.; Zink, J. I.; Brinker, C. J. Mesoporous silica nanoparticle nanocarriers: Biofunctionality and biocompatibility. *Acc. Chem. Res.* **2013**, *46*, 792−801.
(14) Wu, S.-H.; Mou, C.-Y.; Lin, H.-P. Synthesis of mesoporous silica nanoparticles. *Chem. Soc. Rev.* **2013**, *42*, 3862−3875.
(15) Mai, W. X.; Meng, H. Mesoporous silica nanoparticles: A multifunctional nano therapeutic system. *Integr. Biol.* **2013**, *5*, 19−28.
(16) Douroumis, D.; Onyesom, I.; Maniruzzaman, M.; Mitchell, J. Mesoporous silica nanoparticles in nanotechnology. *Crit. Rev. Biotechnol.* **2013**, *33*, 229−245.
(17) Zhang, K.; Xu, L.-L.; Jiang, J.-G.; Calin, N.; Lam, K.-F.; Zhang, S.-J.; Wu, H.-H.; Wu, G.-D.; Albela, B.; Bonneviot, L.; Wu, P. Facile large-scale synthesis of monodisperse mesoporous silica nanospheres with tunable pore structure. *J. Am. Chem. Soc.* **2013**, *135*, 2427−2430.
(18) Wan, Y.; Zhao, D. On the controllable soft-templating approach to mesoporous silicates. *Chem. Rev.* **2007**, *107*, 2821−2860.
(19) Han, L.; Che, S. Anionic surfactant templated mesoporous silicas (AMSs). *Chem. Soc. Rev.* **2013**, *42*, 3740−3752.

(20) Deng, Y.; Wei, J.; Sun, Z.; Zhao, D. Large-pore ordered mesoporous materials templated from non-pluronic amphiphilic block copolymers. *Chem. Soc. Rev.* **2013**, *42*, 4054−4070.
(21) Gérardin, C.; Reboul, J.; Bonne, M.; Lebeau, B. Ecodesign of ordered mesoporous silica materials. *Chem. Soc. Rev.* **2013**, *42*, 4217−4255.
(22) Myers, D. Solid surfaces and dispersions. In *Surfactant Science and Technology*, 3rd ed.; Myers, D., Ed.; Wiley: Hoboken, NJ, 2005; Chapter 10, pp 323−366.
(23) An, K.; Alayoglu, S.; Ewers, T.; Somorjai, G. A. Colloid chemistry of nanocatalysts: A molecular view. *J. Colloid Interface Sci.* **2012**, *373*, 1−13.
(24) Urata, C.; Aoyama, Y.; Tonegawa, A.; Yamauchi, Y.; Kuroda, K. Dialysis process for the removal of surfactants to form colloidal mesoporous silica nanoaprticles. *Chem. Commun.* **2009**, 5094−5096.
(25) Berggren, A.; Palmqvist, A. E. C. Particle size control of colloidal suspensions of mesostructured silica. *J. Phys. Chem. C* **2008**, *112*, 732−737.
(26) Brinker, C. J.; Scherer, G. W. In *Sol-gel Science: The Physics and Chemistry of Sol-Gel Processing*; Brinker, C. J., Scherer, G. W., Eds.; Elsevier: San Diego, CA, 1990; Chapter 3, pp 97−234.
(27) Stöber, W.; Fink, A.; Bohn, E. Controlled growth of monodispersed silica spheres in the micron size range. *J. Colloid Interface Sci.* **1968**, *26*, 62−69.
(28) Yamada, H.; Urata, C.; Aoyama, Y.; Osada, S.; Yamauchi, Y.; Kuroda, K. Preparation of colloidal mesoporous silica nanoparticles with different diameters and their unique degradation behavior in static aqueous systems. *Chem. Mater.* **2012**, *24*, 1462−1471.
(29) Yamada, H.; Urata, C.; Ujiie, H.; Yamauchi, Y.; Kuroda, K. Preparation of aqueous colloidal mesostructured and mesoporous silica nanoparticles with controlled particle size in a very wide range from 20 to 700 nm. *Nanoscale* **2013**, *5*, 6145−6153.
(30) Urata, C.; Yamada, H.; Wakabayashi, R.; Aoyama, Y.; Hirosawa, S.; Arai, S.; Takeoka, S.; Yamauchi, Y.; Kuroda, K. Aqueous colloidal mesoporous nanoparticles with ethenylene-bridged silsesquioxane frameworks. *J. Am. Chem. Soc.* **2011**, *133*, 8102−8105.
(31) Atkin, R.; Craig, V. S. J.; Wanless, E. J.; Biggs, S. Mechanism of cationic surfactant adsorption at the solid−aqueous interface. *Adv. Colloid Interface Sci.* **2003**, *103*, 219−304.
(32) Tyrode, E.; Rutland, M. W.; Bain, C. D. Adsorption of CTAB on hydrophilic silica studied by linear and nonlinear optical spectroscopy. *J. Am. Chem. Soc.* **2008**, *130*, 17434−17445.
(33) Van Der Voort, P.; Ravikovitch, P. I.; De Jong, K. P.; Neimark, A. V.; Janssen, A. H.; Benjelloun, M.; Van Bavel, E.; Cool, P.; Weckhuysen, B. M.; Vansant, E. F. Plugged hexagonal templated silica: A unique micro- and mesoporous composite material with internal silica nanocapsules. *Chem. Commun.* **2002**, 1010−1011.
(34) Kruk, M.; Jaroniec, M.; Joo, S. H.; Ryoo, R. Characterization of regular and plugged SBA-15 silicas by using adsorption and inverse carbon replication and explanation of the plug formation mechanism. *J. Phys. Chem. B* **2003**, *107*, 2205−2213.
(35) Bao, X.; Zhao, X. S.; Li, X.; Li, J. Pore structure characterization of large-pore periodic mesoporous organosilicas synthesized with varying SiO_2/template ratios. *Appl. Surf. Sci.* **2004**, *237*, 380−386.
(36) Van Bavel, E.; Cool, P.; Aerts, K.; Vansant, E. F. Plugged hexagonal templated silica (PHTS): An in-depth study of the structural characteristics. *J. Phys. Chem. B* **2004**, *108*, 5263−5268.
(37) Lu, J. R.; Simister, E. A.; Thomas, R. K.; Penfold, J. Structure of an octadecyltrimethylammonium bromide layer at the air/water interface determined by neutron reflection: Systematic errors in reflectivity measurements. *J. Phys. Chem.* **1993**, *97*, 6024−6033.
(38) Hoshikawa, Y.; Yabe, H.; Nomura, A.; Yamaki, T.; Shimojima, A.; Okubo, T. Mesoporous silica nanoparticles with remarkable stability and dispersibility for antireflective coatings. *Chem. Mater.* **2010**, *22*, 12−14.
(39) Sun, L.; Song, Y.; Wang, L.; Guo, C.; Sun, Y.; Liu, Z.; Li, Z. Ethanol-induced application in DNA detection. *J. Phys. Chem. C* **2008**, *112*, 1415−1422.
(40) Lin, Y.-S.; Abadeer, N.; Hurley, K. R.; Haynes, C. L. Ultrastable, redispersible, small, and highly organomodified mesoporous silica nanotherapeutics. *J. Am. Chem. Soc.* **2011**, *133*, 20444−20457.
(41) Frye, C. L.; Vincent, G. A.; Finzel, W. A. Pentacoordinate silicon compounds. V. Novel silatrane chemistry. *J. Am. Chem. Soc.* **1971**, *93*, 6805−6811.
(42) Cabrera, S.; Haskouri, J. E.; Guillem, C.; Latorre, J.; Beltrán-Porter, A.; Beltrán-Porter, D.; Marcos, M. D.; Amorós, P. Generalised syntheses of ordered mesoporous oxides: The atrane route. *Solid State Sci.* **2000**, *2*, 405−420.
(43) Ikari, K.; Suzuki, K.; Imai, H. Grain size control of mesoporous silica and formation of bimodal pore structures. *Langmuir* **2004**, *20*, 11504−11508.